Journal of Physics: Condensed Matter

Adsorption of Glutamic acid on clean and hydroxylated rutile TiO_2(110): an XPS and NEXAFS investigation

To cite this article before publication: Giovanni Carraro *et al* 2022 *J. Phys.: Condens. Matter* in press https://doi.org/10.1088/1361-648X/ac62a6

Adsorption of Glutamic acid on clean and hydroxylated rutile TiO_2(110): an XPS and NEXAFS investigation

Giovanni Carraro[1,2], Marco Smerieri[1], Simone Passaglia[1], Gianangelo Bracco[1,2], Luca Vattuone[1,2], Mario Rocca[1,2,], Albano Cossaro[3,4], Alberto Verdini[4], Luca Floreano[4], and Letizia Savio[1*]*

[1]IMEM-CNR, U.O.S. Genova, Via Dodecaneso 33, 16146 Genova, IT

[2]Dipartimento di Fisica, Università di Genova, Via Dodecaneso 33, 16146 Genova, IT

[3]Department of Chemical and Pharmaceutical Sciences, University of Trieste, 34127 Trieste, Italy

[4]CNR-IOM, Istituto Officina dei Materiali, 34149 Trieste, Italy

Corresponding authors: rocca@fisica.unige.it , letizia.savio@imem.cnr.it

Abstract:

Due to its biocompatibility, TiO_2 is a relevant material for the study of bio-interfaces. Its electronic and chemical properties are influenced by defects, which mainly consist of oxygen vacancies or adsorbed OH groups and which affect, consequently, also the interaction with biological molecules. Here we report on an X-ray photoemission spectroscopy and Near Edge Adsorption Fine Structure study of glutamic acid (Glu) adsorption on the rutile TiO_2(110) surface, either clean or partially hydroxylated. We show that Glu anchors to the surface through a carboxylate group and that the final adsorption state is influenced by the presence of hydroxyl groups on the surface prior to Glu deposition. Indeed, molecules adsorb both in the anionic and in the zwitterionic form, the former species being favored on the hydroxylated substrate.

Keywords:

Glutamic acid, rutile TiO_2(110), hydroxylation, photoemission spectroscopy, NEXAFS

Introduction:

The organic-inorganic interfaces are most relevant when dealing with biocompatibility issues or pharmacological and hygiene applications. Most often the inorganic surfaces are oxidized and/or hydroxylated since, with the notable exception of gold, metal objects in ambient or biological environment are covered by an oxide or hydroxide layer. Therefore, information is required about the interaction of amino acids with this class of materials, while most of the current studies at the atomic

and molecular level refer to the interface between amino acids and the bare metal surface[1–7]. This is due both to the increased complexity of oxide/hydroxide substrates and to their insulating nature, which prevents the use of electron-based techniques for surface analysis.

TiO_2 represents a fortunate exception in this respect because it combines a semi-conducting nature, precious to avoid charging problems[8], to a high relevance as a biomaterial. It has therefore become the reference oxide for fundamental studies on the interaction of oxide surfaces with biomolecules in general and with amino acids (AA) in particular. Indeed, AA/TiO_2, especially for the monocrystalline rutile TiO_2(110), represents the best system for which the gap between model studies under controlled ultra-high vacuum (UHV) conditions and samples produced in ambient/liquid environment has been bridged.

Adsorption has been studied on TiO_2 for several amino acids[7,9–11] and investigated with an arsenal of techniques ranging from LEED (Low Energy Electron Diffraction), HREELS (High Resolution Electron Energy Loss Spectroscopy), XPS (X-ray Photoemission Spectroscopy), and TPD (Temperature Programmed Desorption, applied to surfaces), to ATR-FTIR (Attenuated Total Reflection-Fourier-Transform Infrared Spectroscopy) and others more convenient for dispersed samples. To the best of our knowledge, only one STM (Scanning Tunnelling Microscope) study has been reported, namely for the Gly/TiO_2(110) 1x1 system[10]. It agrees with photoemission experiments[9] and theoretical models[12] in demonstrating that, at saturation of the first Gly monolayer, the molecules adsorb in form of glycinate and bind to the surface in a μ2 bridge configuration. Indeed, deprotonation of the carboxyl group and formation of Ti-O-C-O-Ti cycles is the most common configuration for the adsorption of carboxylic and bi-carboxylic acids[13,14] and of several amino acids. Additional anchoring points, as well as adsorption as zwitterions, depend then on the molecular species and on the presence of additional functional groups[7].

While model studies tend to consider a perfect substrate, this is not always a good approximation for reality: TiO_2 tends to be defect rich, the most common defects being oxygen vacancies and hydroxyl groups[8,15]. Their presence at the surface may affect the adsorption configuration of the molecules and cannot be neglected for a complete understanding of the system. E.g., a significant role of surface oxygen vacancies was demonstrated for adsorption of arginine[16] and proline[11,17,18] on rutile TiO_2(110). For arginine, DFT calculations inferred that a deficiency of either in-plane oxygen or bridging oxygen weakened the arginine adsorption on the rutile surface. For proline, XPS investigation showed that both a zwitterionic and a deprotonated (anionic) species co-exist. The former is less strongly bound and gets dominant on the reduced surface, most likely because in presence of surface vacancies less oxygen is available at which the dissociated H atom can bind. To

the best of our knowledge, however, much less work has been performed to investigate in a controlled way the effect of the presence of hydroxyls on amino acids adsorption.

Finally, we mention that amino acids with an acidic lateral chain (e.g., aspartic, or glutamic acid) or a basic one (e.g., lysine) have been shown to have affinities with the TiO_2 surfaces[7]. For di-acidic molecules, the interesting question is whether they bind through the α- or the lateral carboxylate functionality, or via both of them. DFT calculations by Guo et al.[19] suggest that the most favourable adsorption configuration for aspartic acid on dry rutile TiO_2(110) in vacuum is the one with both the α-COOH and the NH_2 groups interacting with the surface. The presence of water is predicted to hinder aspartic acid adsorption due to competition for adsorption sites. However, a systematic experimental work confirming this trend is still lacking.

We present here a combined XPS and NEXAFS investigation of the Glu/TiO_2(110) system performed under controlled UHV conditions for the clean and for the hydroxylated surface. Besides characterising the molecule-surface interaction at different temperatures, we demonstrate that the adsorption state of the admolecules significantly depends on the initial condition of the substrate. Due to the presence of hydroxyls on the TiO_2 surface under real conditions, we believe that the fundamental understanding of the effect of such contamination on the adsorption properties of a biological molecule as glutamic acid is a key issue of practical interest.

Experimental:

The first set of X-ray photoemission (XPS) experiments was performed in Genova, in an apparatus hosting a conventional, non-monochromatic X-ray source (DAR400, Omicron) and a hemispherical analyzer (EA125, Omicron) for photoemission spectroscopy; in addition, the apparatus is equipped with a four degrees of freedom manipulator, a home-made evaporator suitable for organic molecules and all other typical vacuum facilities, including a quadrupole mass spectrometer for residual gas analysis, an ion gun and leak-valves for gas inlet. The second set of XPS data and NEXAFS spectra were recorded at the ALOISA beamline[20] in Trieste (Elettra Synchrotron, Italy), which is equipped with a preparation chamber hosting similar vacuum facilities.

In both cases the sample was cooled down by liquid N_2 flux and could be heated to T = 1000 K either by irradiation or electron bombardment. While annealing samples covered by Glu, electron bombardment was avoided since it was proven to cause partial fragmentation of the admolecules.

In Genova, XPS spectra were recorded at normal emission and using a conventional, non-monochromatic $Mg_{K\alpha}$ excitation source (hν = 1256.6 eV). At ALOISA, they were acquired in Transverse-Magnetic polarization and near normal emission with a homemade hemispherical

analyzer (R = 66 mm, acceptance angle of 1.5°) equipped with a 2-dimensional delay-line detector developed by Elettra. We used photon energies hν = 650 eV, 510 eV, and 140 eV (with overall resolution of 280 meV, 160 meV and 120 meV, respectively) to measure the spectra [O 1s + Ti 2p + N 1s + C 1s + Ti 3p], [N 1s + C1s + Ti 3p] and [Ti 3p + VB], respectively.

All the spectra are calibrated on the reference binding energy of Ti $2p_{3/2}$ (E_b = 459.1 eV) and/or Ti 3p (E_b = 37.6 eV). The sets of XPS data recorded in Genova and at ALOISA are perfectly compatible and, except for the valence band region, we show here the former investigation because it is more complete.

NEXAFS spectra at the N and C *K*-edge were measured in partial electron yield by means of a channeltron equipped with a grid, which is negatively polarized to filter out secondary electrons at energy lower than the KLL Auger lines of N and C (-370 V and -250 V, respectively). The sample is illuminated at constant grazing angle (4° and 6° for XPS and NEXAFS, respectively), while the orientation with respect to linearly polarized electric field direction is changed from Transverse-Magnetic (TM, or quasi p-polarization) to Transverse-Electric (TE, or s-polarization) by rotating the sample around the photon beam axis, thanks to the coaxial manipulator. The photon energy resolution was set to 75 and 90 meV for NEXAFS measurements at the C and N *K*-edge, respectively. A posteriori, we performed an absolute energy calibration (±20 meV) of the NEXAFS spectra by recording simultaneously the drain current (i_0) on the last mirror[21]. For spectra normalization, we also measured reference NEXAFS spectra on the clean substrate.

Two different TiO_2(110) single crystal samples (10 mm × 5 mm, Mateck) were employed in the different apparatuses. Since our analysis is focused on the role of sample defectivity, we took particular care in selecting samples of similar color, since this is the signature of a similar amount of F centers in the bulk. The rutile TiO_2(110) surfaces were prepared by cycles of Ar^+ sputtering (1.0 keV) followed by annealing to 920 K. The annealing process is known to restore surface order and to heal the oxygen vacancies created by sputtering through segregation of oxygen atoms from the bulk[8]. In some cases, a subsequent treatment consisting in annealing to 473 K in O_2 pressure ($5 \cdot 10^{-7}$ mbar for 5 minutes, corresponding to 100 L of exposure) was also performed. As shown in the valence band spectra of Figure 1, the effect of this additional treatment is to remove the OH contamination on the surface prior to Glu deposition. In the following we will refer to the surface as "pristine" ($TiO_2(110)_p$) or OH-contaminated ($TiO_2(110)_{hydro}$) depending on whether it was annealed in oxygen to remove OH or if traces of OH are still present in the VB spectra. Glu was eventually evaporated by resistively heating the crucible to T_{ev}=400 K while keeping the sample at the desired temperature 250 K ≤ T ≤ 400 K. In both experimental chambers the base pressure was better than $1 \cdot 10^{-9}$ mbar and raised to a maximum of $5 \cdot 10^{-9}$ mbar during Glu evaporation.

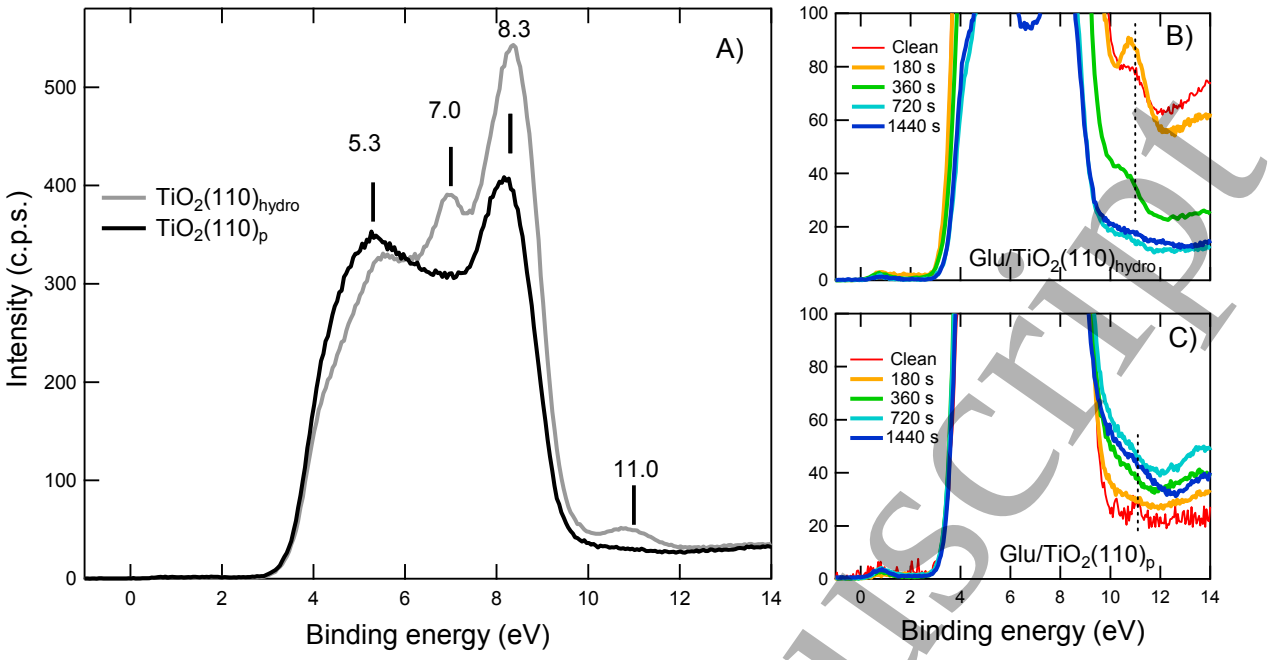

Fig. 1. A) Valence band spectra of the pristine and OH-contaminated TiO_2(110) surface before Glu deposition. For the latter, the presence of hydroxyls is evident from the intensity at 11 eV and from the additional feature around 7.0 eV due to the O 2p bands[15,22]. B) and C) Enlargement of the VB spectra showing the evolution of the OH signal around 11 eV with increasing Glu exposure. All spectra of each series are normalized on the photocurrent. We observe that the OH signal in panel B increases with the first Glu dose and reduces thereafter. This non-monotonic behavior derives from the combination of two effects. Some additional water may adsorb on the surface during the very first stages of Glu deposition, when most of the surface is still bare. With increasing Glu coverage the OH signal reduces, possibly due to H_2 formation and desorption, as discussed later in the text.

Data analysis is performed using the KolXPD software for the fitting of the XPS spectra, and with IgorPro software for data treatment and presentation. Photoemission spectra are fitted with Voigt functions after background subtraction. Typical XPS data and the relative analysis are shown in Fig. 2. Panel A) shows the O 1s intensity recorded for the pristine and OH-contaminated surface prior to Glu adsorption. Both spectra present a major component at E_b = 530.4 eV, associated with the O ions of the oxide lattice, and a smaller one at 531.9 eV, which can be related to the unresolved contributions of surface oxygen atoms and OH groups[23]. The latter peak is larger for $TiO_2(110)_{hydro}$, while the corresponding Ti 2p spectrum (not shown) presents a significant decrease of the Ti^{3+} component at 457 eV, related to defect sites (see the following). Therefore, the overall picture supports the VB information that a larger amount of hydroxyl groups are present at the surface in this case and that the oxygen treatment has the effect of removing OH and filling oxygen vacancies, hence reducing the defectivity in the topmost layer of the crystal.

After Glu deposition (panel B), the 530.4 eV peak remains unchanged while the high E_b one grows and shifts to 532.1 eV due to the contribution of O atoms of the amino acid layer[7,24]. However, it is still significantly smaller with respect to the TiO_2 component, so that a quantitative analysis would be difficult and subject to large errors. For these reasons, we are not going to deal with O 1s spectra in our further analysis.

The Ti 2p region shows the typical Ti 2p doublet at 459.1 eV and 464.8 eV and smaller components at 457.0 eV and 462.7 eV, corresponding to Ti^{3+} ions and indicating the presence of a small number of O vacancies in the first few layers of the crystal.

Two components (N1 and N2) are necessary to reproduce the N 1s region, while three are employed to fit the C 1s one (C1 to C3); their nature is discussed later in the text.

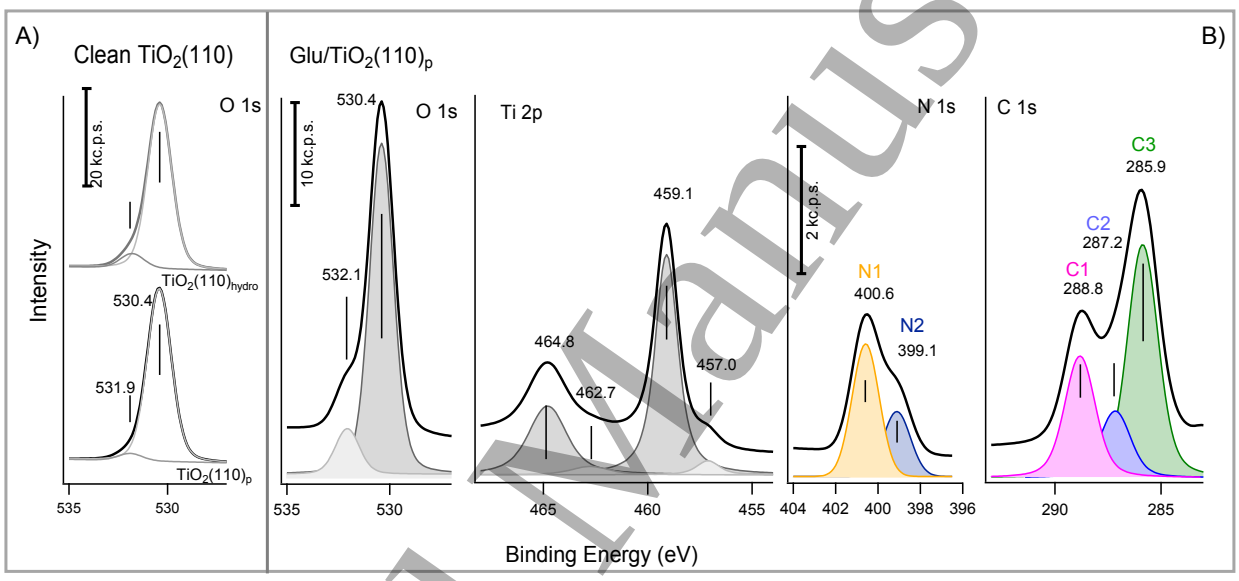

Fig. 2. A) Photoemission spectra of the O 1s region for pristine and OH-contaminated TiO_2(110) surface prior to Glu deposition. B) Photoemission spectra of O 1s, Ti 2p, N 1s, and C1s regions after 960 s of deposition of Glu on the $TiO_2(110)_p$ surface at T = 300 K (corresponding to saturation coverage). Black dots are the raw data after background subtraction, the continuous black line is the best fit to the data and the colored curves represent the different components. Binding energies are determined with an accuracy of ±0.1 eV.

Results:

Fig. 3 compares the outcome of two Glu uptake experiments performed at room temperature (RT) on the pristine (left panels) and OH-contaminated (right panels) TiO_2(110) surface. In both cases, the total intensity in the C 1s and N 1s regions increases with time, as indicated by the curves in Fig. 4 (left column). A reduction in the adsorption rate is observed for exposure times t > 480 s and suggests that the first monolayer of Glu is almost saturated and that multilayers are not likely to form at RT.

This behavior is in agreement with what was already observed for Glu on Ag surfaces[4,25] and for most amino acids both on metals and oxide surfaces[7,26].

Focusing the attention on the pristine surface, we notice that the C1s peak consists of three components at 288.8 eV, 287.7 eV, and 285.9 eV (C1, C2, and C3 in the following- see table 1). From comparison with published literature, we assign C3 to the unresolved photoemission signals of C atoms bound to H and N, C2 to C atoms in carboxylate (COO^-) groups, and C1 to C atoms in carboxylic (COOH) groups[7]. The presence of carboxylate suggests that adsorption occurs with the deprotonated acidic group as the main anchoring point, similarly to what already reported for other amino acid species[7] (see sketch in Fig. 3B). Of course, alternative interpretations can be conjectured; e.g. C1 could correspond to the unresolved contributions of the carboxylic and carboxylate groups, while C2 and C1 could be due to the α-C and aliphatic C atoms, respectively. We believe that this hypothesis is much less plausible since the stochiometric ratio among the peaks should be 2:1:2, contrary to experimental evidence. Furthermore, the α-C is reported to be at E_b<287 eV both for amino acids on metal surfaces[7] and for Phe and Pro on rutile $TiO_2(110)$[11,24].

The N 1s region initially shows a broad and rather flat intensity ranging from ~398.5 eV to ~401 eV, which evolves in a well resolved superposition of two main components: N1 at E_b ~ 400.5 eV and N2 at 399.0 eV (see table 1 and Fig. 2B). Since each Glu molecule has only one amino group, this is indicative that the molecules adsorb in two different conformations on the surface, as discussed in the following. The relative ratio between the N 1s lines changes with increasing exposure, the N1 species becoming dominant at the largest doses.

Interestingly, the twin experiment performed on $TiO_2(110)_{hydro}$ yields the same spectral components, but with different relative weights. Now the C2 peak clearly emerges in the C 1s region and dominates over C1. Even more striking, the ratio between the N1 and N2 components in the N1s region is reversed, the 399.0 eV peak being now almost twice as high as the 400.6 eV one for any dose longer than t = 60 s. The different behavior of the two surfaces with respect to Glu uptake is evidenced by the curves in Fig. 4 (right column), which report the intensity of the single C 1s (top panel) and N 1s (bottom panel) components for the two series of spectra of Fig. 3.

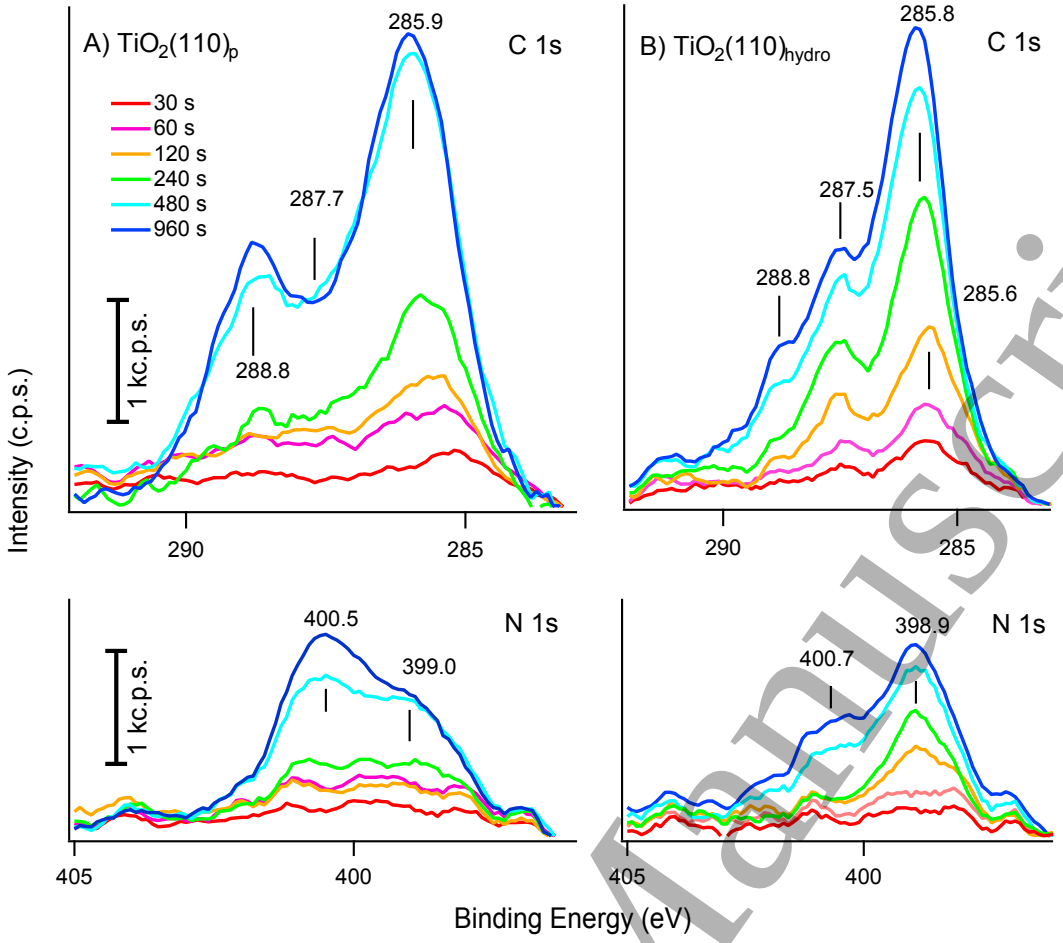

Fig. 3 XPS spectra of the C 1s and N 1s regions recorded after increasing Glu exposures with the sample at T = 300 K on $TiO_2(110)_p$ and $TiO_2(110)_{hydro}$. *Here and in the following figures the spectrum corresponding to the clean TiO_2 surface is subtracted to remove the background.*

A sketch of the anchoring geometry, with the carboxylate group forming a Ti-O-C-O-TI bridge, is reported in panel B.

Component	E_b (eV)	Assignment
C 1s		
C1	288.8±0.1	COOH
C2	287.5±0.3	COO^-
C3	285.8±0.1	α-C; aliphatic C
N 1s		
N1	400.6±0.1	NH_3^+
N2	399.0±0.1	NH_2

Table 1. Summary of the C 1s and N 1s components detected in the experiments.

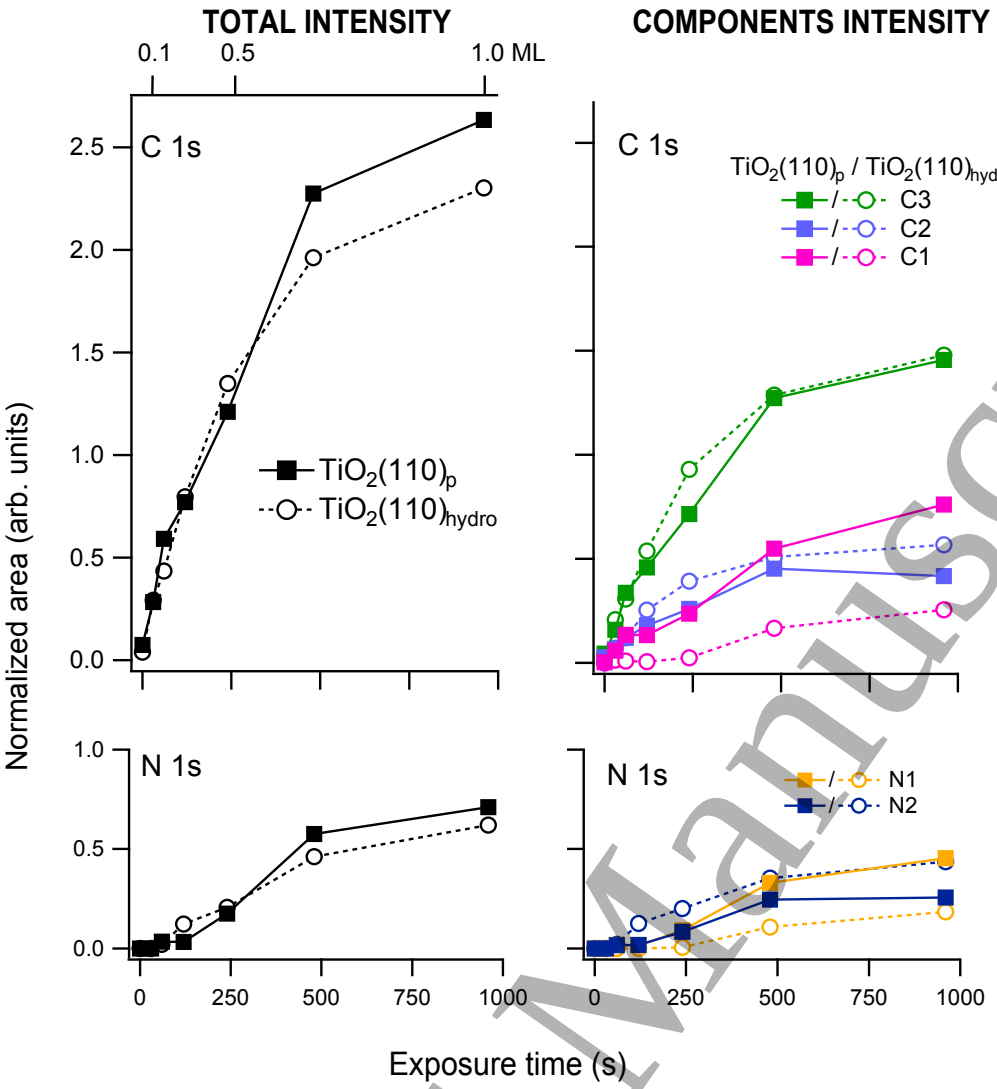

Fig. 4 Left: Total area of the C 1s and N 1s photoemission signals vs exposure time for the uptake experiments reported in Fig. 3 on the pristine and OH-contaminated $TiO_2(110)$ surface, respectively. The top axis indicates the approximate Glu coverage based on the C1s intensity and considering the 960 s dose close to the saturation coverage of 1 ML. Right: Area of C 1s and N 1s components vs exposure time calculated for the same spectra. The error on each point is ~10% of the corresponding value for the smallest XPS signals and reduces to ~5% for the more intense peaks.

To characterize Glu adsorption in better detail, we deposited Glu on the pristine substrate for 240 s, a dose corresponding to sub-monolayer coverage at RT, at temperatures ranging from 250 K up to 393 K. XPS spectra of C 1s and N 1s regions are shown in Fig. 5 and show that the signal intensity decreases with increasing T. Since the dose is the same for all conditions, this means that at lower temperature the residence time of the molecules on the surface increases so that diffusion of the physisorbed precursor becomes favored over the competing desorption process; hence the probability to reach the proper site for stable adsorption becomes larger. Experimentally, we observe that the

sticking coefficient of Glu on TiO_2(110) is temperature dependent and we deduce that a precursor mediated adsorption mechanism is active, similarly to what previously reported for different Ag surfaces[4,27].

Both the C 1s and N 1s regions are best described by the C1-C3 and N1-N2 components discussed above and summarized in Table 1. We note, however, that their relative intensity depends on the deposition temperature. In particular, C1 is smaller or comparable to C2 for exposures at or above room temperature (RT) while it is larger at 250 K. The N 1s components present a more complex behaviour. Starting from the preparation at 300 K, we have already noted (see Fig. 3) that the two components have comparable intensity. Upon deposition at higher T, the N1 line faints, while the N2 one remains almost constant, suggesting that it is associated with a thermally more stable Glu form. The N2 component represents indeed almost 80% of the total N 1s intensity under such conditions. At T = 250 K, on the contrary, both lines get more intense due to the increased sticking probability. Again, the N2 peak dominates, indicating that this species is more populated, resembling the spectrum recorded at RT on the hydroxylated surface. This behavior is possibly due to some OH contamination occurring at low T during or immediately before the dose.

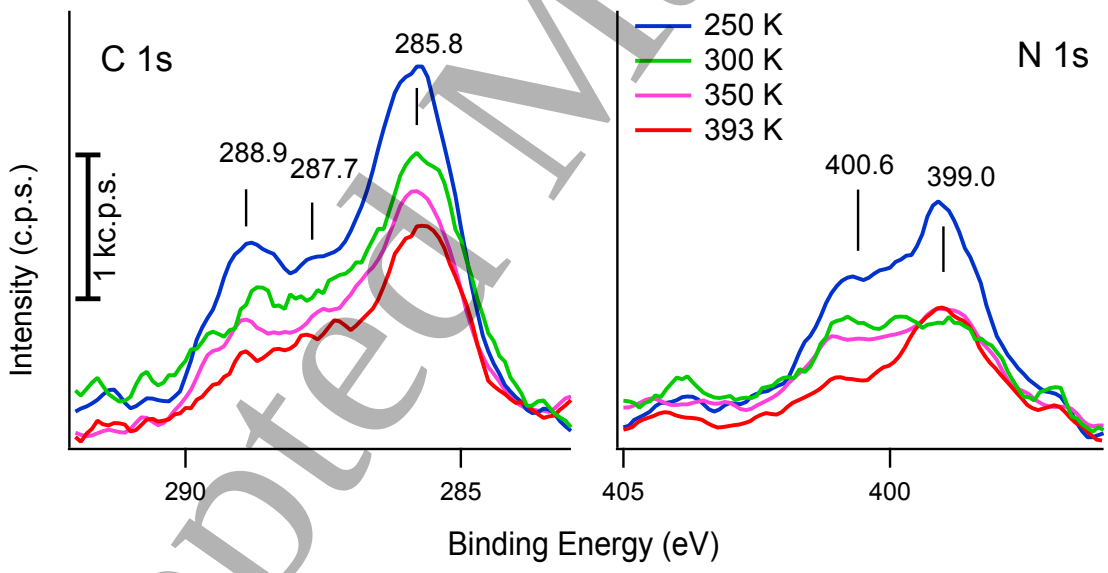

Fig. 5 XPS spectra of the C1s and N1s regions after the adsorption of Glu on pristine TiO_2(110) at different T. The exposure time is 240 s in all cases.

Fig. 6 shows the thermal evolution of the 250 K layer of Fig. 5. The decrease in the intensity of the C 1s and N 1s spectra after annealing to 300 K, 325 K and 350 K indicates a progressive desorption of the molecules, which is more evident when heating from 250 K to RT. Both the C 1s and the N 1s spectra present the same components observed in the previous experiments, though the binding

energies tend towards slightly lower values at lower coverage. Also in this case, the lower thermal stability of the N1 component with respect to N2 is confirmed.

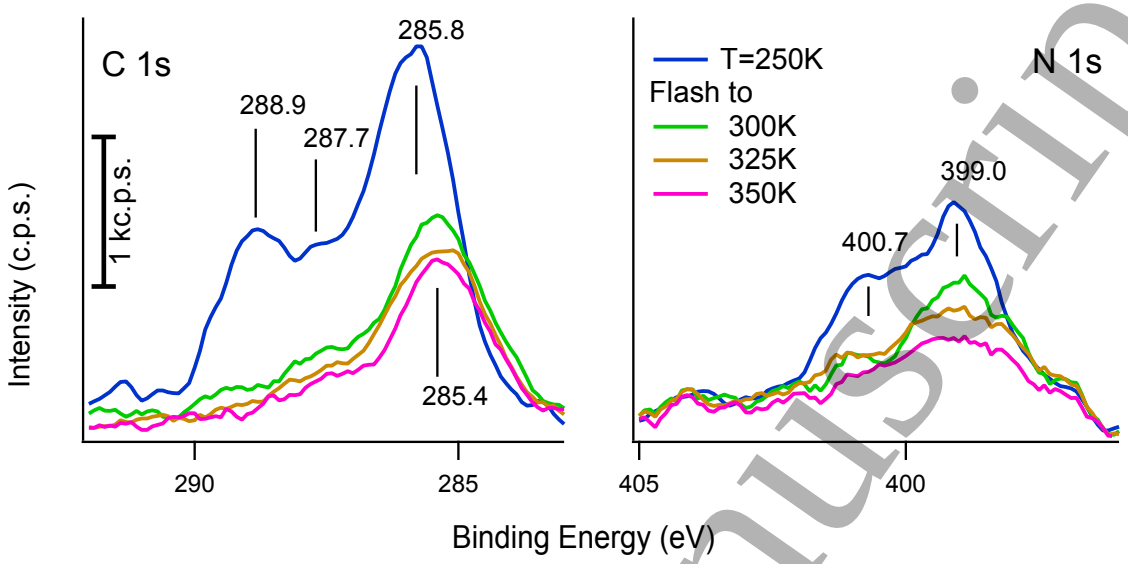

Fig. 6. XPS spectra of the C1s and N1s regions after the adsorption of Glu on the pristine TiO_2(110) substrate at T=250 K (exposure time of 240 s) and subsequent annealing to higher temperature.

The XPS data of Fig. 3 are complemented by recording NEXAFS spectra in s- and p-polarization of the C and N K-edge on both $TiO_2(110)_p$ and $TiO_2(110)_{hydro}$ samples. The spectra corresponding to saturation coverage are reported in Fig. 7.

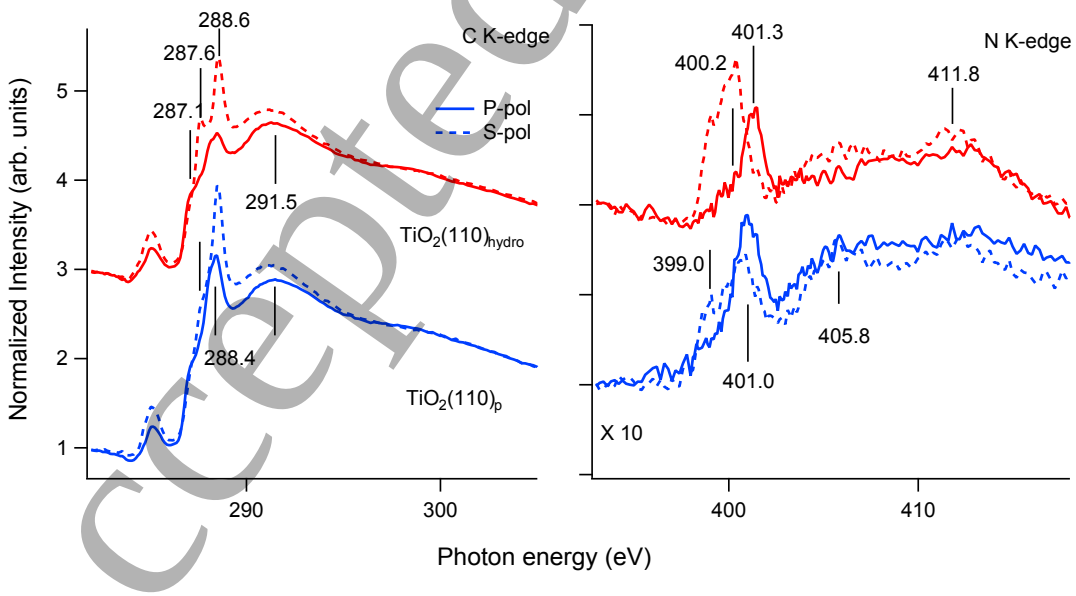

Fig. 7. NEXAFS spectra of the C and N K-edge recorded at saturation coverage of Glu on pristine (bottom spectra) and OH-contaminated (top spectra) rutile TiO_2(110) surfaces at 300 K. Spectra

taken with either the Magnetic field (TM) or the Electric field (TE) transverse to the scattering plane, corresponding to quasi p-polarization and exactly s-polarization, respectively (see Experimental section for details).

The C region presents at least three C 1s → π* resonances in the energy range between 287.1 eV and 288.6 eV and a broad C 1s → σ* resonance around 291 eV. The N region shows three N 1s → π* resonances between 399.0 eV and 401.3 eV and two broad σ* resonances around 405.8 eV and 411.8 eV. The shape and intensity of these features depend on polarization, thus indicating at least a partial orientation of the molecular bonds. In addition, spectra recorded with the same polarization for the pristine and OH-contaminated samples present some differences, suggesting adsorption in different molecular conformations. Focusing on the C K-edge region, we first observe the modification of the transition at 288.6 eV, which is sharp and intense in s-polarization, broader and slightly downshifted in p-polarization. This behavior suggests that it consists indeed of two unresolved contributions showing opposite dichroism. The 288.6 eV peak emerges in s-polarization and can be safely assigned to the C 1s → π* transition of the C atoms involved in the carboxylate functionality by comparison with other amino acid and bi-carboxylic acid systems. Indeed, such transition has been found at 288.6 eV for Ala/Cu(412)[28], for Cys/Au(110)[29] and for Cys/Cu(531)[28], around 288.5 eV for L-Tyr/Ag(111)[29] and at 288.8 eV for malonic acid on rutile TiO_2(110)[14]. The dependence of this peak on surface polarization indicates that the final state orbital is oriented at a small angle with respect to the surface plane, which is coherent with the adsorption of the molecule through the carboxylate group, possibly in a bridge configuration. The unresolved component at lower energy, on the contrary, is almost negligible in s-polarization. This is indicative of a preferential C bond orientation nearly parallel to the surface, to be associated to the radical tail of the amino acid. The non-dichroic feature around 291 eV is most probably due to the contributions to the C 1s → σ* resonance of both the C-C and C-N single bonds[29], which are expected to be at a lower energy compared to C-O double bonds[30]. Finally, an additional peak at 287.6 eV is present only in s-polarization and only for the bare sample.

Moving to the N K-edge region, the broad peaks around 405.8 eV and 411.8 eV, more defined in s-polarization, are identified with the transition of the 1s electrons of the N atoms to σ*(C-N) resonances[31]. Three features are visible in the energy region typical of N 1s → π* resonances at 399.0 eV, 400.2 eV and 401.3 eV: the peaks at 399.0 eV and 400.2 eV are much more intense in s- than in p-polarization; vice versa, the one around 401 eV is more intense in p-polarization. This behavior suggests a preferential orientation of the amino group which may be different for the two nitrogen species detected by XPS.

If we compare the NEXAFS spectra obtained on the two samples, we note that the energies of the resonance peaks are similar, but their relative intensities may differ significantly, thus confirming the different relative population of the adsorption sites already observed by XPS.

Discussion

Our data compare the adsorption of glutamic acid on rutile TiO_2(110) in presence or in absence of a limited hydroxylation of the substrate, which forms spontaneously due to the interaction with water molecules present in the residual atmosphere of the UHV chamber. We mention that the evidence of surface hydroxylation comes from a careful inspection of the valence band, which is possible only for the data recorded at the ALOISA beamline. For this reason we could not complement our data with additional experiments in which the surface is deliberately hydroxylated by controlled H_2O exposure.

Though a precise quantification of the OH coverage is not straightforward, there is a general experimental agreement that water dissociation occurs on TiO_2(110) at RT only at oxygen vacancies at the bridging oxygen rows[8,15]. It has also been demonstrated that population of such defect by an OH group does not affect the intensity of the defect state observed at 0.9 eV, coherently with our data of Fig. 1[15,32]. Therefore, based on the intensity of the Ti^{3+} 2p signal (component at 457 eV in Fig. 2), which provides information on the density of defective sites averaged over the first layers of the sample, and on comparison with other studies[22,33] we estimate an OH coverage lower than 10%.

Due to the presence of hydroxyls on the TiO_2 surface under real conditions, the understanding of the effect of such contamination on the adsorption properties of biological molecules, such as glutamic acid, becomes of high practical interest.

By comparing the uptake curves of Fig. 4, we first note that, at the largest doses, the total intensity in the C 1s and N 1s regions is ~10% higher for the pristine sample, indicating a larger availability of adsorption sites in absence of OH.

As mentioned in the introduction, the favorite adsorption configuration for amino acids at TiO_2(110) is the μ2 one[7], in which the two oxygen atoms of the carboxylate group bind to adjacent Ti atoms forming a Ti-O-C-O-Ti bridge (see sketch in Fig. 3B). Though additional anchoring points may be present depending on the nature of the molecule, this configuration holds not only for amino acids but for organic acids in general[13,14]. In case of bi-carboxylic acids, the open question is whether they anchor to the surface through one or both carboxyl groups. Looking at the relative intensity of the C 1s components, we can draw some conclusions on this point for Glu/TiO_2(110). First, we note that the 3:2 ratio expected between (aliphatic + α) C atoms (C3 component) and C atoms in carboxylic or carboxylate groups (C1 and C2) is well respected for both samples; this reinforces our assignment of

the three components. Secondly, the C1/C2 ratio is ~1.8 and ~0.7 for the pristine and OH-contaminated samples, respectively, meaning that full deprotonation of the carboxylic groups does not occur and that the fraction of deprotonated groups is larger for the OH-contaminated surface. Therefore, our data suggest that the molecules anchor to the surface with only one carboxylate group; for analogy with other amino acid species, most probably it is the one connected to the α-C, which binds in a bridge configuration[7,34,35]. This hypothesis is coherent with the NEXAFS information that the carboxylate group associated to the 288.6 eV resonance is oriented nearly normal to the surface.

Another interesting and correlated issue is the different population of the N1 and N2 species in the N 1s spectrum which depends on the surface condition. There is a general agreement in scientific literature that binding energies in the range of 399 eV - 400 eV correspond to the amino group in the neutral form while the zwitterion is characterized by $E_b \geq 400.5$ eV[7,11,34]. By analogy with previous results, we therefore assign the N1 peak to the NH_3^+ species and the N2 one to NH_2. The assignment is reinforced by the observed thermal behavior of the Glu layer, since other amino acids in the zwitterionic form are reported to be less stable that the corresponding anionic species[18]. This leads to the conclusion that Glutamic acid adsorbs on rutile $TiO_2(110)$ at RT both in the anionic and in the zwitterionic form. From the area of the different N 1s components we estimate that, close to saturation coverage, approximately 2/3 of the molecules adsorb as zwitterions on the pristine surface while this fraction reduces to 1/3 on $TiO_2(110)_{hydro}$. Dissociation of the molecule is thus favored by OH pre-coverage. This behavior is unexpected since, for anionic adsorption of amino acids at $TiO_2(110)$, the dissociated H atom is likely to bind to a bridging oxygen of the surface[36], so that dissociation should be favored if more bridging oxygens are available. E.g., in the case of Proline[17] adsorption in the zwitterionic form is privileged in presence of O-vacancies while the anionic species prevails on the stochiometric surface.

The opposite behavior observed here suggests that the presence of OH groups at the surface makes dissociation energetically favorable with respect to zwitterionic adsorption. Though we do not have a quantitative explanation for this behavior, we can observe that OH groups are polar, so that their interaction with a neutral NH_2 group or with a charged NH_3^+ is probably quite different. Moreover, the formation of possible hydrogen bonds between the amino groups and the nearby bridging oxygen atoms is inhibited. This may affect both the molecular conformation and chemical state. Indeed, NEXAFS spectra recorded at RT for saturation coverage of Glu are different on the two surfaces. Furthermore, the C/N ratio determined from XPS spectra at saturation coverage is (2.8±0.5) for $TiO_2(110)_p$ and (4.5±0.5) for $TiO_2(110)_{hydro}$. The latter value is compatible with the stochiometric ratio of 5. The former, on the contrary, indicates a lack of carbon which can be justified in term of partial screening of the molecular backbone by an upstanding amino group and/or by photoelectron

diffraction effects. In both cases, this result points at a change in the adsorption conformation of the Glu units.

Finally, we can speculate about the destiny of the dissociated H atoms. It is reasonable that they bind to a bridging oxygen as in the case of glycine[36]. The alternative possibility that they adsorb at the 5-fold coordinated Ti atoms is improbable, since this site was demonstrated to be significantly less stable for adsorption of atomic hydrogen[37]. Recombinative desorption as a water molecule is ruled out since it is reported only above 500 K [15]; moreover, it would imply the formation of bridging oxygen vacancies and the consequent increase of the Defect State intensity in the gap at ~0.9 eV, contrary to experimental evidence (see Fig. 1B-C). Conversely, recombination as H_2 is controversial since some authors observed it already at 240 K while others did not report it to occur[15]. This mechanism is however the most likely because the VB measurements as a function coverage indicate that the OH concentration at the $TiO_2(110)_{hydro}$ surface (peak at ~11 eV binding energy in Fig. 1B) decreases gradually above a critical Glu exposure and vanishes at the completion of the monolayer. Thus, we suggest that the presence of a surface hydroxyl nearby a Glu molecule favors the hydrogen release from the carboxylic termination to the adjacent O_{br} rows, possibly suggesting an OH pairing. As the Glu coverage increases, the hydroxyls recombine to H_2 leaving the surface.

Conclusions:

We have reported here on a XPS and NEXAFS study on the adsorption of Glu on pristine and OH-contaminated rutile $TiO_2(110)$. Glu molecules adsorb at RT both in the zwitterionic and in the anionic form, anchoring to the surface through a carboxylate group, which is oriented at a small angle with respect to the surface normal. The presence of pre-adsorbed OH affects the adsorption state of the molecules, the zwitterionic form being more abundant in absence of OH and the anionic one dominating on the partially hydroxylated surface.

Considering the relevant role of TiO_2-based materials as the inorganic part of bio-interfaces and their typical applications in humid environment, we believe that a deeper insight in the way the presence of contaminants in general, and of OH in particular, affects the adsorption of biomolecules is essential for their full exploitation.

Acknowledgment: We thank Jagriti Pal and Angelique Lusuan for their contribution in the initial stages of the experiment. We acknowledge financial support from MIUR through projects PRIN2017 n. 2017NYPHN8 and n. 2017KFMJ8E_003, from Fondazione Compagnia di S. Paolo through project MC-nano. We acknowledge Elettra Sincrotrone Trieste for providing access to its synchrotron radiation facilities and for financial support.

References:

(1) Barlow, S. M.; Raval, R. Complex Organic Molecules at Metal Surfaces: Bonding, Organisation and Chirality. *Surf. Sci. Rep.* **2003**, *50* (6–8), 201–341. https://doi.org/10.1016/S0167-5729(03)00015-3.

(2) Kühnle, A.; Linderoth, T. R.; Besenbacher, F. Chiral Symmetry Breaking Observed for Cysteine on the Au(110)-(1×2) Surface. *Top. Catal.* **2011**, *54* (19–20), 1384–1391. https://doi.org/10.1007/s11244-011-9765-z.

(3) Jones, T. E.; Baddeley, C. J.; Gerbi, A.; Savio, L.; Rocca, M.; Vattuone, L. Molecular Ordering and Adsorbate Induced Faceting in the Ag{110}−(S)-Glutamic Acid System. *Langmuir* **2005**, *21* (21), 9468–9475. https://doi.org/10.1021/la050414b.

(4) Smerieri, M.; Vattuone, L.; Kravchuk, T.; Costa, D.; Savio, L. (S)-Glutamic Acid on Ag(100): Self-Assembly in the Nonzwitterionic Form. *Langmuir* **2011**, *27* (6), 2393–2404. https://doi.org/10.1021/la1033993.

(5) Schiffrin, A.; Riemann, A.; Auwarter, W.; Pennec, Y.; Weber-Bargioni, A.; Cvetko, D.; Cossaro, A.; Morgante, A.; Barth, J. V.; Auwärter, W.; Pennec, Y.; Weber-Bargioni, A.; Cvetko, D.; Cossaro, A.; Morgante, A.; Barth, J. V. Zwitterionic Self-Assembly of L-Methionine Nanogratings on the Ag(111) Surface. *Proc. Natl. Acad. Sci.* **2007**, *104* (13), 5279–5284. https://doi.org/10.1073/pnas.0607867104.

(6) Gao, F.; Li, Z.; Wang, Y.; Burkholder, L.; Tysoe, W. T. Chemistry of Glycine on Pd(111): Temperature-Programmed Desorption and X-Ray Photoelectron Spectroscopic Study. *J. Phys. Chem. C* **2007**, *111* (27), 9981–9991. https://doi.org/10.1021/jp071943m.

(7) Costa, D.; Pradier, C. M.; Tielens, F.; Savio, L. Adsorption and Self-Assembly of Bio-Organic Molecules at Model Surfaces: A Route towards Increased Complexity. *Surf. Sci. Rep.* **2015**, *70* (4), 449–553. https://doi.org/10.1016/j.surfrep.2015.10.002.

(8) Diebold, U. The Surface Science of Titanium Dioxide. *Surf. Sci. Rep.* **2003**, *48* (5), 53–229. https://doi.org/10.1016/S0167-5729(02)00100-0.

(9) Soria, E.; Colera, I.; Roman, E.; Williams, E. .; de Segovia, J. L. A Study of Photon-Induced Processes with Adsorption-Desorption of Glycine at the TiO2(110)(1×2) Surface. *Surf. Sci.* **2000**, *451* (1–3), 188–196. https://doi.org/10.1016/S0039-6028(00)00026-1.

(10) Qiu, T.; Barteau, M. A. STM Study of Glycine on TiO2(110) Single Crystal Surfaces. *J. Colloid Interface Sci.* **2006**, *303* (1), 229–235. https://doi.org/10.1016/j.jcis.2006.07.053.

(11) Fleming, G. J. J.; Adib, K.; Rodriguez, J. A. A.; Barteau, M. A. A.; Idriss, H. Proline

Adsorption on TiO2(110) Single Crystal Surface: A Study by High Resolution Photoelectron Spectroscopy. *Surf. Sci.* **2007**, *601* (24), 5726–5731. https://doi.org/10.1016/j.susc.2007.06.074.

(12) Ojamäe, L.; Aulin, C.; Pedersen, H.; Käll, P.-O. IR and Quantum-Chemical Studies of Carboxylic Acid and Glycine Adsorption on Rutile TiO2 Nanoparticles. *J. Colloid Interface Sci.* **2006**, *296* (1), 71–78. https://doi.org/10.1016/j.jcis.2005.08.037.

(13) Gutiérrez-Sosa, A.; Martínez-Escolano, P.; Raza, H.; Lindsay, R.; Wincott, P. L.; Thornton, G. Orientation of Carboxylates on TiO2(110). *Surf. Sci.* **2001**, *471* (1–3), 163–169. https://doi.org/10.1016/S0039-6028(00)00902-X.

(14) Syres, K. L.; Thomas, A. G.; Graham, D. M.; Spencer, B. F.; Flavell, W. R.; Jackman, M. J.; Dhanak, V. R. Adsorption and Stability of Malonic Acid on Rutile TiO2 (110), Studied by near Edge X-Ray Absorption Fine Structure and Photoelectron Spectroscopy. *Surf. Sci.* **2014**, *626*, 14–20. https://doi.org/10.1016/j.susc.2014.03.015.

(15) Henderson, M. The Interaction of Water with Solid Surfaces: Fundamental Aspects Revisited. *Surf. Sci. Rep.* **2002**, *46* (1–8), 1–308. https://doi.org/10.1016/S0167-5729(01)00020-6.

(16) Zhang, H.; Lu, X.; Luo, X.; Lin, X.; Zhou, Y. Effects of O-Deficiency on the Interaction between Rutile and Arg: A Density Functional Theory Study. *Phys. E Low-dimensional Syst. Nanostructures* **2014**, *61*, 83–89. https://doi.org/10.1016/j.physe.2014.03.017.

(17) Fleming, G. J.; Adib, K.; Rodriguez, J. A.; Barteau, M. A.; White, J. M.; Idriss, H. The Adsorption and Reactions of the Amino Acid Proline on Rutile TiO2(110) Surfaces. *Surf. Sci.* **2008**, *602* (12), 2029–2038. https://doi.org/10.1016/j.susc.2008.04.010.

(18) Fleming, G. J.; Idriss, H. Probing the Reaction Pathways of DL-Proline on TiO2 (001) Single Crystal Surfaces. *Langmuir* **2004**, *20* (18), 7540–7546. https://doi.org/10.1021/la049492.

(19) Guo, Y.; Lu, X.; Zhang, H.; Weng, J.; Watari, F.; Leng, Y. DFT Study of the Adsorption of Aspartic Acid on Pure, N-Doped, and Ca-Doped Rutile (110) Surfaces. *J. Phys. Chem. C* **2011**, *115* (38), 18572–18581. https://doi.org/10.1021/jp200598t.

(20) Floreano, L.; Naletto, G.; Cvetko, D.; Gotter, R.; Malvezzi, M.; Marassi, L.; Morgante, A.; Santaniello, A.; Verdini, A.; Tommasini, F.; Tondello, G. Performance of the Grating-Crystal Monochromator of the ALOISA Beamline at the Elettra Synchrotron. *Rev. Sci. Instrum.* **1999**, *70* (10), 3855–3864. https://doi.org/10.1063/1.1150001.

(21) Bavdek, G.; Cossaro, A.; Cvetko, D.; Africh, C.; Blasetti, C.; Esch, F.; Morgante, A.; Floreano, L. Pentacene Nanorails on Au(110). *Langmuir* **2008**, *24* (3), 767–772. https://doi.org/10.1021/la702004z.

(22) Walle, L. E.; Borg, A.; Uvdal, P.; Sandell, A. Experimental Evidence for Mixed Dissociative and Molecular Adsorption of Water on a Rutile TiO_2 (110) Surface without Oxygen Vacancies. *Phys. Rev. B - Condens. Matter Mater. Phys.* **2009**, *80* (23), 1–5. https://doi.org/10.1103/PhysRevB.80.235436.

(23) Bullock, E. L.; Patthey, L.; Steinemann, S. G. Clean and Hydroxylated Rutile TiO2(110) Surfaces Studied by X-Ray Photoelectron Spectroscopy. *Surf. Sci.* **1996**, *352–354* (95), 504–510. https://doi.org/10.1016/0039-6028(95)01188-9.

(24) Thomas, A. G.; Flavell, W. R.; Chatwin, C. P.; Kumarasinghe, A. R.; Rayner, S. M.; Kirkham, P. F.; Tsoutsou, D.; Johal, T. K.; Patel, S. Adsorption of Phenylalanine on Single Crystal Rutile TiO2(1 1 0) Surface. *Surf. Sci.* **2007**, *601* (18), 3828–3832. https://doi.org/10.1016/j.susc.2007.04.085.

(25) Tranca, I.; Smerieri, M.; Savio, L.; Vattuone, L.; Costa, D.; Tielens, F. Unraveling the Self-Assembly of the (S)-Glutamic Acid "Flower" Structure on Ag(100). *Langmuir* **2013**, *29* (25), 7876–7884. https://doi.org/10.1021/la4012923.

(26) Cavalleri, O.; Gonella, G.; Terreni, S.; Vignolo, M.; Floreano, L.; Morgante, A.; Canepa, M.; Rolandi, R. High Resolution X-Ray Photoelectron Spectroscopy of l-Cysteine Self-Assembled Films. *Phys. Chem. Chem. Phys.* **2004**, *6* (15), 4042. https://doi.org/10.1039/b405516k.

(27) Smerieri, M.; Vattuone, L.; Rocca, M.; Savio, L. Spectroscopic Evidence for Neutral and Anionic Adsorption of (S)-Glutamic Acid on Ag(111). *Langmuir* **2013**, *29* (23), 6867–6875. https://doi.org/10.1021/la400436r.

(28) Thomsen, L.; Tadich, A.; Riley, D. P.; Cowie, B. C. C.; Gladys, M. J. Investigating the Enantioselectivity of Alanine on a Chiral Cu{421} R Surface. *J. Phys. Chem. C* **2012**, *116* (17), 9472–9480. https://doi.org/10.1021/jp207847j.

(29) Reichert, J.; Schiffrin, A.; Auwärter, W.; Weber-Bargioni, A.; Marschall, M.; Dell'Angela, M.; Cvetko, D.; Bavdek, G.; Cossaro, A.; Morgante, A.; Barth, J. V.; Auwärter, W.; Weber-Bargioni, A.; Marschall, M.; Dell'Angela, M.; Cvetko, D.; Bavdek, G.; Cossaro, A.; Morgante, A.; Barth, J. V. l-Tyrosine on Ag(111): Universality of the Amino Acid 2D Zwitterionic Bonding Scheme? *ACS Nano* **2010**, *4* (2), 1218–1226. https://doi.org/10.1021/nn901669p.

(30) Hasselström, J.; Karis, O.; Nyberg, M.; Pettersson, L. G. M.; Weinelt, M.; Wassdahl, N.; Nilsson, A. The Bonding and Electronic Structure Changes upon Adsorption of Important Functional Groups: Glycine on Copper. *J. Phys. Chem. B* **2000**, *104* (48), 11480–11483. https://doi.org/10.1021/jp000986z.

(31) Feyer, V.; Plekan, O.; Tsud, N.; Cháb, V.; Matolín, V.; Prince, K. C. Adsorption of Histidine and Histidine-Containing Peptides on Au(111). *Langmuir* **2010**, *26* (11), 8606–8613. https://doi.org/10.1021/la904684e.

(32) Di Valentin, C.; Pacchioni, G.; Selloni, A. Electronic Structure of Defect States in Hydroxylated and Reduced Rutile TiO_2(110) Surfaces. *Phys. Rev. Lett.* **2006**, *97* (16), 166803. https://doi.org/10.1103/PhysRevLett.97.166803.

(33) Lovat, G.; Forrer, D.; Abadia, M.; Dominguez, M.; Casarin, M.; Rogero, C.; Vittadini, A.; Floreano, L. On-Surface Synthesis of a Pure and Long-Range-Ordered Titanium(IV)-Porphyrin Contact Layer on Titanium Dioxide. *J. Phys. Chem. C* **2017**, *121* (25), 13738–13746. https://doi.org/10.1021/acs.jpcc.7b03157.

(34) Ataman, E.; Isvoranu, C.; Knudsen, J.; Schulte, K.; Andersen, J. N.; Schnadt, J. Adsorption of L-Cysteine on Rutile TiO_2(110). *Surf. Sci.* **2011**, *605* (1–2), 179–186. https://doi.org/10.1016/j.susc.2010.10.017.

(35) Li, C.; Monti, S.; Ågren, H.; Carravetta, V. Cysteine on TiO2(110): A Theoretical Study by Reactive Dynamics and Photoemission Spectra Simulation. *Langmuir* **2014**, *30* (29), 8819–8828. https://doi.org/10.1021/la5014973.

0(36) Lerotholi, T. J.; Kröger, E. A.; Knight, M. J.; Unterberger, W.; Hogan, K.; Jackson, D. C.; Lamont, C. L. A.; Woodruff, D. P. Adsorption Structure of Glycine on TiO2(1 1 0): A Photoelectron Diffraction Determination. *Surf. Sci.* **2009**, *603* (15), 2305–2311. https://doi.org/10.1016/j.susc.2009.05.009.

(37) Kunat, M.; Burghaus, U.; Wöll, C. The Adsorption of Hydrogen on the Rutile TiO2(110) Surface. *Phys. Chem. Chem. Phys.* **2004**, *6* (16), 4203–4207. https://doi.org/10.1039/b404629c.